PCCP

Probing electron transfer dynamics of pyranine with reduced graphene oxide

Journal:	*Physical Chemistry Chemical Physics*
Manuscript ID:	CP-ART-07-2014-003225.R1
Article Type:	Paper
Date Submitted by the Author:	13-Aug-2014

Complete List of Authors:	Kathiravan, Arunkumar; University of Madras, National Centre for Ultrafast Processes jcs, Nithya; National Institute of Technology, Trichy, Centre for Energy and Environmental Science and Technology Mariadoss, Asha Jhonsi; B.S. Abdur Rahman University, Chemistry

Cite this: DOI: 10.1039/c0xx00000x

www.rsc.org/xxxxxx

ARTICLE TYPE

Probing electron transfer dynamics of pyranine with reduced graphene oxide

M. Asha Jhonsi[a], C. Nithya[b], A. Kathiravan[c]*

Received (in XXX, XXX) Xth XXXXXXXXX 20XX, Accepted Xth XXXXXXXXX 20XX

DOI: 10.1039/b000000x

A stable reduced graphene oxide (rGO) was prepared and characterized by X-ray diffraction (XRD) and Laser Raman spectroscopy. A steady state and time-resolved fluorescence quenching studies have been carried out to elucidate the process of electron transfer from excited pyranine (POH) into the rGO dispersion. POH adsorbed strongly on rGO dispersion with an apparent association constant of 33.4 $(mg/ml)^{-1}$, and its fluorescence emission was quenched with an apparent association constant of 33.7 $(mg/ml)^{-1}$. Picosecond lifetime measurements gave the rate constant for the electron transfer process from the excited singlet state of POH into the rGO dispersion is 8.8 x 10^9 s^{-1}. Laser flash photolysis studies demonstrated the formation of radicals for the evidence of electron transfer between POH and rGO.

Introduction

Graphene is a two-dimensional (2-D) nanomaterial consisting of sp^2-hybridized carbon that can be exfoliated from bulk graphite and it has drawn the much interest of scientists in recent years.[1-3] However, the applications of graphene have been hindered by its poor processibility. This problem can be overcome by the functionalization on the graphene sheet surface by Hummers method.[4] After reacting with strong oxidants, graphene oxide (GO) with hydroxyl, epoxyl and carboxyl groups on the sheet surface can be obtained.[5] The presence of these functional groups makes the individual GO sheets suspendable in both polar and nonpolar solvents but severely decreases the conductivity as a result of a loss in the conjugated sp^2 network. In this regard, hydrazine has been used to reduce GO and increase the conductivity by restoring the sp^2-hybridized network. Other reductants such as $NaBH_4$ and hydroquinone have also been used.[6,7] All of these reduction approaches allow only partial restoration of the sp^2 network, and the product is commonly referred to as reduced graphene oxide (rGO). Since the reduced graphene oxide exhibits many physical properties similar to that of graphene, they are being considered in for the construction of next-generation flexible solar-energy-conversion and optoelectronic devices that are low-cost, high-efficiency, thermally stable, environmentally friendly, and lightweight.[8]

With the increasing attention to energy and environmental issue, many researchers focus on solar cell, which has potential application in our daily life. An electron transfer from a sensitizer to electrode materials (such as TiO_2 nanoparticles) is a fundamental process, which could strongly influence the efficiency of solar cells. Incorporation of graphene sheets into TiO_2 nanoparticle films used as photoanodes in dye-sensitized solar cells gave five times higher power conversion efficiencies than those obtained with TiO_2 nanoparticle films without graphene sheets.[9] First time, Imahori et al. developed an efficient hierarchical ET cascade system on a semiconducting electrode in a bottom-up manner by using rGO as a 2D sheet to anchoring organic/inorganic hybrid materials. The deposited film exhibited remarkably high photocurrent generation (IPCE = 70%) compared with the reference device without rGO sheets.[10] Therefore, the interaction studies and electron injection dynamics of sensitizer adsorbed GO sheets would be very important. The interaction of graphene with aromatic dyes, such as phthalocyanine, pyrenebutyrate, porphyrin, eosin, methylene blue, F27, pyrene, fluorescein and rhodamine B has been reported.[11] In most of these cases the quenching was proposed to occur via photo-induced electron transfer was reported.[12] However, no general consent about the nature and origin of the quenching of sensitizer fluorescence by graphene has been recognized so far. Here, we have investigated the photophysical properties of pyranine (POH) in the presence of reduced graphene oxide (rGO) to understand the fundamental processes such as ground state association and electron transfer.

Pyranine (8-hydroxypyrene-1,3,6-trisulfonate, POH, **Scheme 1**) is the class of pyrene derivative. Recently Thomas et al. developed pyrene-based organic dyes with thiophene containing π-linkers for dye-sensitized solar cells. The power conversion efficiency of metal-free organic dyes containing pyrene is of 3.3%.[13a] Very recently, Song et al. reported a novel tetrahydropyrene-based D–π–A organic dye for the first time, featuring 4,5,9,10-tetrahydropyrene as a π-conjugation linker to bridge between the diphenylamine unit and the thienyl acrylic acid moiety.[13b] It exhibited power conversion efficiency of 6.75%. So, it is worth to explore the photophysical processes of

pyrene derivatives in solution as well as on materials. In this direction, very recently, Pal et al. reported the excited state electron transfer from aminopyrene to rGO.[14] They have shown that rGO is effectively quenching the fluorescence of aminopyrene and the quenching is due to photoinduced electron transfer from aminopyrene to rGO. Moreover, they have shown that the lack of ground state complex formation between them. For an efficient photoanode, dye should adsorb on rGO via complex formation. Keeping mind that, the present work focuses on ground state association and electron transfer studies of POH and rGO by using Uv-Vis absorption, steady state and time resolved fluorescence spectroscopy.

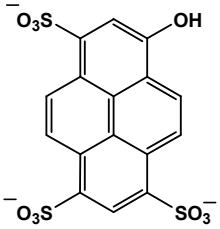

Scheme 1: Structure of Pyranine

2. Materials and Methods

8-Hydroxypyrene-1,3,6-trisulfonic acid (POH) was purchased in Aldrich, India. For the synthesis of reduced Graphene Oxide (rGO), we started from the synthesis of Graphene Oxide (GO) from graphite powder through modified Hummers method[4,15]. Graphite powder (2 g, Alfa Aesar>99%) and $NaNO_3$ (1g; Merck >99%) were mixed, then transferred this mixture into concentrated H_2SO_4 (96 ml; Merck, 98%) with an ice bath. $KMnO_4$ (6 g; Merck > 99%) was added gradually under vigorous stirring and maintain the temperature of the mixture was below 20°C. The ice bath was removed, and then the mixture was stirred at 35°C in a water bath for 18 h. As the reaction proceeds, we observed the brownish color pasty mixture and subsequently 150 ml of water was added to this pasty mixture. But this reaction is highly exothermic in nature because addition of water into concentrated H_2SO_4 will liberate large amount of heat so the mixture should be kept in an ice bath while adding water and keep the temperature below 50°C. Further diluting with 240 ml of water 5 ml of 30% H_2O_2 was added to this mixture and the diluted solution colour changed to sparkling yellow along with bubbling. Under continuous stirring for 2 h, the mixture was filtered and washed thoroughly with 10% aqueous HCl solution (250 ml; Merck), deionized water and ethanol (Merck) to remove other ions[16]. Finally the resulting mass was dried by vacuum. The reduced graphene oxide was prepared through simple reduction method using $NaBH_4$ as a reducing agent. In a typical experiment, 1g of GO was dispersed in 50 ml of distilled water using ultrasound in an ultrasonic bath (Model PCi analtics, 230 V, 50 Hz) for 1hr. To this solution, 0.02 mole of $NaBH_4$ was added drop by drop under continuous stirring and again exposed to ultrasound for 30 min, and then collected the black colour solid by filtration. The resulting solid was dried in oven for 1h and subjected to structural characterization. The synthesized GO and rGO were characterized by using a x–ray diffractometer ('Xpert PRO PANalytical PW 3040/60 'X'Pert PRO') at a scan rate of $1°min^{-1}$ using Cu–K_α radiation (λ = 1.5418Å), while the voltage and current were held at 40 kV and 20 mA (2θ = 5–80°) respectively. Laser Raman spectra were recorded for the synthesized materials in a WITec Confocal Raman Instrument with Ar ion laser (wavelength 514.5 nm, power – 50%).

For spectroscopic studies, the triple distilled water was used for preparing the solutions. The absorption spectra of samples were recorded using an Agilent 8453 UV-visible diode array spectrophotometer. The fluorescence spectral measurements were carried out using Fluoromax-4 spectrophotometer (Horiba Jobin Yvon). For fluorescence studies, very diluted solutions were used to avoid spectral distortions due to the inner-filter effect and emission reabsorption. Time-resolved fluorescence decays were obtained by the time correlated single-photon counting (TCSPC) technique exciting the sample at 390 nm. The typical full width at half-maximum (FWHM) of the system response using a scatterer is about 50 ps. Data analysis was carried out by the software provided by IBH (DAS-6), which is based on deconvolution techniques using nonlinear least-squares method and the quality of the fit is ascertained with the value of $\chi^2 < 1.2$. Transient absorption experiments were carried out using nanosecond laser flash photolysis (Applied Photophysics, UK). Transient absorption experiments were carried out using nanosecond laser flash photolysis (Applied Photophysics, UK). The third harmonic (355 nm) of a Q-switched Nd:YAG laser (Quanta-Ray, LAB 150, Spectra Physics, USA) with 8 ns pulse width and 150 mJ pulse energy was used to excite the samples. The transients were probed using a 150W pulsed xenon lamp, a Czerny-Turner monochromator, and Hamamatsu R-928 photomultiplier tube as detector. The transient signals were captured with an Agilent 500MHz 1GSa/s Infiniium Oscilloscope, and the data were transferred to the computer for further analysis.

3. Results and Discussion

Structural features of rGO

Figure 1 compares the XRD patterns of GO and rGO (synthesized by $NaBH_4$ reduction method). As seen in XRD pattern of GO, the main 2θ peak (002) is centered at 10. 8° which is consistent with previously reported literature[17].

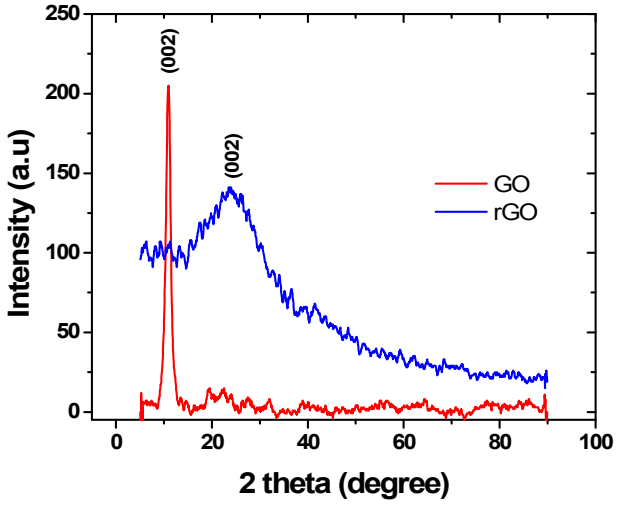

Figure 1. XRD patterns of GO and rGO

After reduction of GO using $NaBH_4$, the (002) plane of GO shifted to higher angle i.e 2θ = 24. 89° indicates that the formation of rGO[18] as we can clearly seen from the XRD pattern of rGO. The obtained XRD pattern of rGO matches well with the reported literature.[19] Absence of peak at 2θ = 10.8° in the XRD pattern of rGO ascribes that the reducing agent completely reduces the GO phase.

Laser Raman scattering is one of the sensitive tool to analyze the graphene based materials[20]. Generally the Raman spectra of graphene based materials show two major bands[21] i.e D (κ point phonons of A1g symmetry) and G band (phonons of E_{2g} symmetry) which distinguish the vibration of defect related sp^3 bonded carbon atoms and sp^2 carbon atoms respectively. D band is historically known as disorder band which arises due to lattice motion away from the center of the Brillouin zone. Its presence between 1270 and 1450 cm^{-1} which depends on the excitation wavelength indicates defects or edges in the graphene based materials.[22] In-plane motion of carbon atoms is the main spectral feature of graphenes and it is extremely sensitive to strain effects and also a good indicator of number of graphene layers. As the number of layers increases, this G band shift to lower frequencies. However, 2D band is usually use to determine the number of layers in graphene.[23] **Figure 2** depicts the Laser Raman spectra of GO and rGO materials. D and G bands centered at 1327 and 1598 cm^{-1} for GO and 1335 and 1596 cm^{-1} for rGO respectively. In GO, D and G bands appeared equal in intensity however, after the reduction process the internsity of D band increases as compared to D band of GO is attributed to the formation of defects. The intensity ratio of D/G for GO is 1.03 and for rGO is 1.29 respectively. The increase in intensity with broader as well as stronger D band suggests that the high degree of disorder presents in graphene layers results more defects[24] which were created during functionalization process of GO. The second order 2D band is usually appeared at 2700 cm^{-1} which is useful to determine the number of graphene layers however, in the present case appears as hump and this is much useful to understand the electronic effects of graphene related materials[20,25]. The weak intensity of this 2D band is due to the splitting of electronic band structure of multi-layer reduced graphene oxides.[26] The increase in intensity and broadening of D band generated more defects in the rGO matrixes which increases the conductivity.

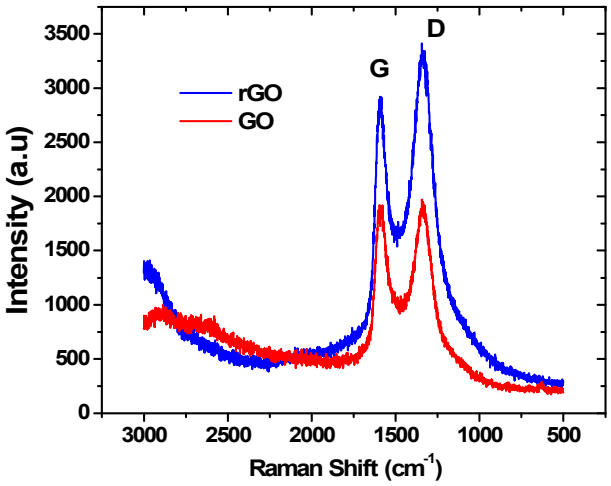

Figure 2. Laser Raman spectra of GO and rGO

Photophysics of POH in solution

POH is known to excited state proton transfer reactions (ESPT).[27] The ESPT dynamics of pyranine has been previously established in various media. It was found that ESPT occurs only in water or in aqueous mixtures containing large fraction of water.[28] Therefore, detailed understanding of POH photophysics in solution is very necessary while studying the electron transfer reactions between POH and reduced graphene oxide (rGO), in this approach we have studied the steady state and time-resolved fluorescence of POH in water medium. Generally, pyrene molecules are very prone to form aggregation in solution. So, first we have investigated the aggregation behavior of POH in water by using absorption spectroscopy. As the POH concentration is increased, the intensity of POH absorbance increased and there were no new bands observed **(figure S1a)**. At the same time, Beer-Lambert law is obeyed for POH in the concentration ranges from 4 μM to 40 μM showing that the POH not significantly aggregated within this concentration range (**figure S1b**). The extinction coefficient value of POH is 2.3 x 10^4 $M^{-1}cm^{-1}$. Moreover, we have investigated the proton transfer properties of POH in ground state. For that we have chosen another solvent namely acetonitrile (ACN). Since the solubility of POH in acetonitrile is very poor; it is dissolved in water and then the solution was diluted with acetonitrile (in 95% acetonitrile + 5% water).

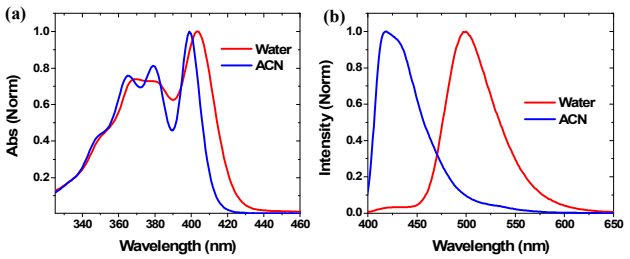

Figure 3: (a) Absorption spectra of POH in water (red line) and in acetonitrile (blue line); (b) Emission spectra of POH in water (red line) and in acetonitrile (blue line).

Figure 3a shows the absorption spectra of POH in water and acetonitrile. The spectra exhibits a peak at ~ 405 nm which is ascribed to the protonated form at the same time as no absorption band for the deprotonated form (PO^-) is observed which is normally appeared at 450 nm.[27] It clearly indicates that there is no proton transfer in the ground state. By comparing acetonitrile and water, later shows 10 nm red shifted, this is due to high polarity of the medium. Moreover, by changing pH from natural to basic, we can able to see the deprotonated form of pyranine at 450 nm (**figure S2**). This figure clearly reveals that the appearance of deprotonated form. This finding is quite relevant for the present work, because when we adding rGO dispersion to the solution of POH, the solution pH may vary as a result spectral shift must be observed. However for POH…rGO system, there is no peak observed at 450 nm. It clearly indicates that there is no deprotonation occurs when it adsorb on rGO. The detailed discussion will come under following section. **Figure 3b** shows the emission spectra of POH in water and acetonitrile. In acetonitrile, we observed a strong emission at 425 nm, based on the report we assigned this peak comes from protonated form,

this further indicates that only the protonated form exists in the excited state, in acetonitrile medium. However in water, very strong emission observed at 515 nm which is ascribed to deprotonated emission. Moreover, the protonated emission is completely quenched; this is due to the occurrence of ESPT reaction to water. This observation can be further verified by time resolved fluorescence measurements.

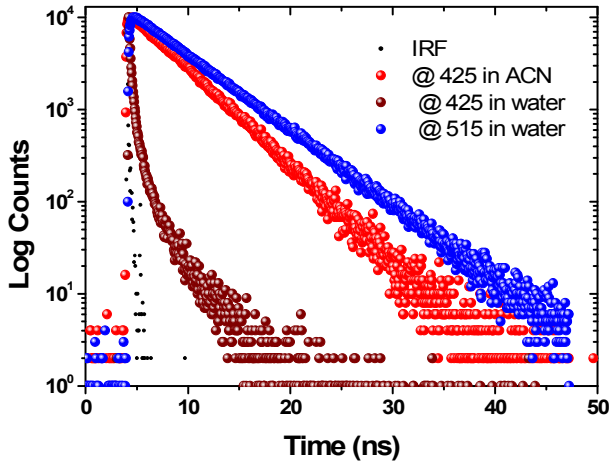

Figure 4: Time resolved fluorescence decay of POH in acetronitrile and in water.

Figure 4 shows the time resolved fluorescence decay of POH monitored at both protonated (425 nm) and deprotonated emission (515 nm) respectively. In acetonitrile, POH exhibits single exponential fluorescence decay with the lifetime of 4.4 ns and the absence of emission at 515 nm (where the deprotonated form emits) is observed, it clearly evident that there is no ESPT from POH to acetonitrile. However, in water medium the dynamics of POH is different with respect to monitoring wavelengths. The fluorescence decay of POH monitored (where deprotonated form emits) at 515 nm results a single exponential decay with the lifetime of 5.2 ns and the decay of weak protonated emission (at 425 nm) is fitted to a tri-exponential with time constants of 116 ps (48%) and additional slow components of 800 ps (34%) and 1800 ps (18%). This confirmed that the existence of excited-state proton-transfer of POH to water. In summary of the photophysics, perhaps the most striking result is that the ESPT is observed in water medium whereas the same has not found in acetonitrile medium.

Absorption characteristics of POH with rGO

Reduced graphene oxide (rGO) dispersed only in water, so we have carry out the measurements in water medium. **Figure 3a** depicted the absorption spectrum of POH with varying concentration of rGO. While increasing concentration of rGO, the POH absorbance getting enhanced, moreover no spectral shift was observed. This clearly reveals that there is a ground state complex[29] between them; moreover the solution pH remains the same as evidenced by absence of spectral shift. The formation of such complex can be explained by the following equation (1):

$$POH + rGO \overset{K_{app}}{\rightleftharpoons} POH....rGO \qquad \rightarrow (1)$$

The changes in optical density of the absorption spectrum of POH as a result of the formation of complex, it can be utilized to obtain apparent association constant (K_{app}) according to the equation (2) reported by Benesi and Hildebrand.[30]

$$\frac{1}{A_{obs}-A_0} = \frac{1}{A_c-A_0} + \frac{1}{K_{app}(A_{obs}-A_0)[rGO]} \qquad \rightarrow (2)$$

Where, A_{obs} is the observed absorbance of POH containing different concentrations of rGO, A_0 and A_c are the absorbance of POH and the complex (POH…rGO) respectively. If the enhancement of absorbance at 403 nm is due to absorption of surface complex, we would expect a linear relationship between $1/(A_{obs}-A_0)$ and the reciprocal concentration of rGO with a slope equal to $1/K_{app}(A_c-A_0)$ and an intercept equal to $1/(A_c-A_0)$. **Figure 3b** shows the Benesi-Hildebrand plot to determine the apparent association constant (K_{app}) of the complex, and the value 33.4 $(mg/ml)^{-1}$. Similar kinds of rGO association with various organic molecules were reported in the literature.[31]

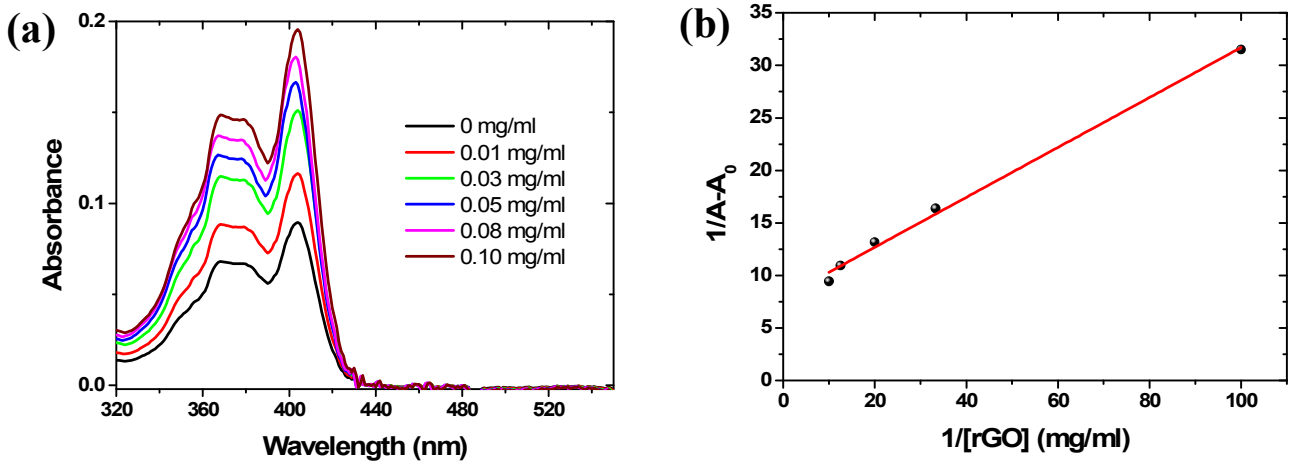

Figure 5: (a) Absorption spectrum of POH (4×10^{-6} M) in the absence and presence of rGO dispersion, (b) Linear dependence of $1/A-A_0$ on the reciprocal concentration of rGO.

Cite this: DOI: 10.1039/c0xx00000x

www.rsc.org/xxxxxx

ARTICLE TYPE

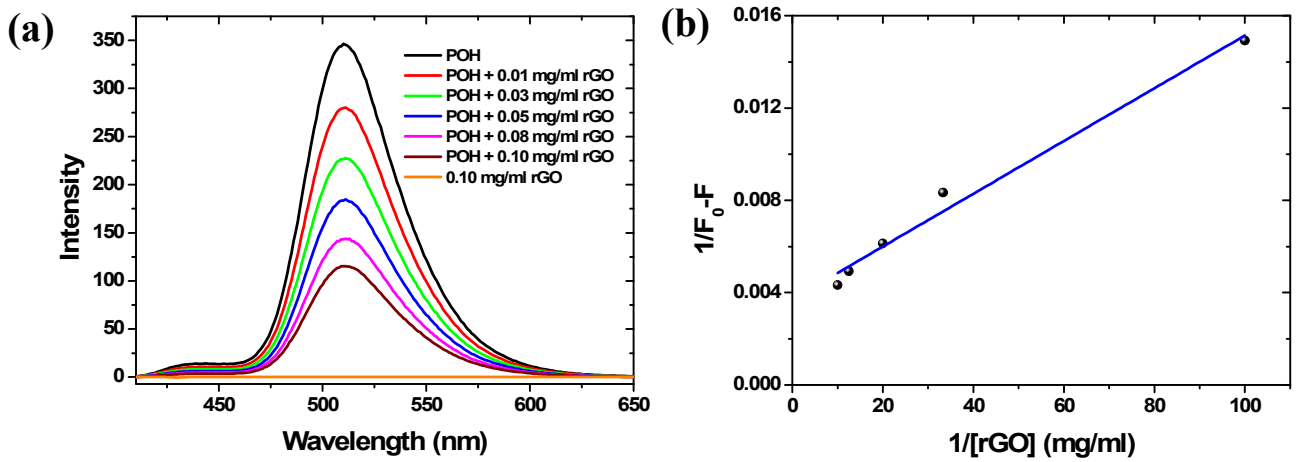

Figure 4: (a) Emission spectrum of POH (4×10^{-6} M) in the absence and presence of rGO dispersion, (b) Linear dependence of $1/F_0$-F on the reciprocal concentration of rGO.

Emission characteristics of POH with rGO

The aptitude of rGO to interact with excited states of molecules and semiconductor nanoparticles is a topic of current research interest. Such interactions often entail energy and electron transfer processes. The emission of the excited molecule serves as an excellent probe to monitor the interactions and thus establish a quenching pathway. Based on this context, we have studied the fluorescence quenching of POH with varying rGO concentrations, which is depicted in **figure 4a**. In the absence of rGO, POH exhibits very weak emission at 425 nm and a strong emission at 515 nm, which are ascribed to protonated and deprotonated forms. However, upon addition of rGO to POH results quenching of its fluorescence intensity and there is no change in the shape of the emission spectrum, even with the highest concentration of the rGO used. This signifies the fact that there is no emitting exciplex formation upon addition of rGO.

Quenching of the fluorescence intensity of the POH is analyzed using Stern–Volmer relationship (3):

$$I_0/I = 1 + Ksv\,[Q] \qquad \rightarrow (3)$$

Where, I_0 and I are the fluorescence intensities of POH in the absence and presence of the rGO and K_{SV} is the quenching constant. The plot between I_0/I and [Q] is non-linear **(plot not shown here).** The deviation of I_0/I from linearity is due to the presence of both static quenching and dynamic quenching. The static quenching is owing to the formation of ground state complex (POH…rGO) as shown in the absorption spectral studies, while the dynamic quenching is attributed to the free POH. The free POH involved in the ESPT reactions as a result we could see the emission spectrum at 515 nm. This can further verified by using time resolved fluorescence spectroscopy, will come under section.

Assuming that, static quenching plays a major role in the quenching of fluorescence of POH by rGO (i.e.) strong π–π interactions[29] between POH and rGO. So, one can determine the apparent association constant from fluorescence quenching data using equation (4),[32]

$$\frac{1}{F_0\text{-}F} = \frac{1}{F_0\text{-}F'} + \frac{1}{K_{app}(F_0\text{-}F')[rGO]} \qquad \rightarrow (4)$$

where, F_0 is the initial fluorescence intensity of free POH, F′ is the fluorescence intensity of POH…rGO complex and F is the observed fluorescence intensity at its maximum. The plot between $1/(F_0\text{-}F)$ and the reciprocal concentration of rGO gives a straight line **[Figure 4b]** and from the slope we have calculated the K_{app} value and is 33.7 $(mg/ml)^{-1}$. Moreover, the obtained K_{app} value from fluorescence studies is exactly matches with the K_{app} obtained from absorption spectral studies. The good agreement between these K_{app} values highlighted the strength of assumption proposed for the association between POH and rGO.

Mechanism of quenching

The decrease in fluorescence emission may be attributed to electron transfer or energy transfer process. The possibility of energy transfer process from POH to rGO can be easily ruled out due to the absence of overlap between the fluorescence spectrum of POH with the absorption spectrum of rGO [spectrum not shown here]. So, from the above discussion we confirmed that the fluorescence quenching could be caused by the electron transfer.[33] The stepwise electron transfer mechanism has been depicted in **scheme 2**.

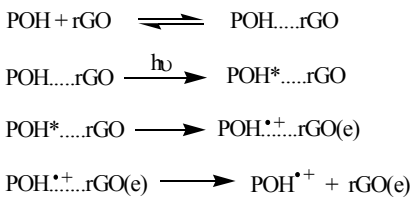

Scheme 2: Mechanism of electron transfer quenching process

This electron transfer quenching is needs to further verify by time resolved fluorescence spectroscopy. Moreover, electron injection from the excited singlet POH to rGO can be anticipated from the estimated oxidation potential of the ^{1}(POH)* (–1.99 V), which is lower than the reported Fermi level of the rGO (0 V). This difference in the energy levels should be sufficient to drive the electron transfer from excited POH to the rGO.

Electron injection dynamics

Fluorescence lifetime can be obtained by measuring fluorescence decay using time resolved fluorescence technique. Measurement of fluorescence lifetime[34] is useful to monitor the electron transfer process from the dyes to oxide surface and carbon based materials. It has been shown earlier[35] that the sensitizer molecules adsorbed on oxide surface had a significantly shorter lifetime when compared with sensitizer alone and the decrease of lifetime was correlated with an electron transfer process. So, in the present work, we have employed time correlated single photon counting technique to perceive the fluorescence lifetime of POH with and without rGO. The fluorescence decay of POH in the absence and presence of rGO is shown in **figure 5**. In the absence of rGO, the fluorescence decay of POH can be fitted to a single exponential expressed as [$F(t) = A \exp(-t/\tau)$] with lifetime of 5.2 ns. However in presence of rGO, the fluorescence decay of POH is shortened and it can be fitted to a bi-exponential decay [$F(t) = A_1 \exp(-t/\tau_1) + A_2 \exp(-t/\tau_2)$], with short-lived and longer-lived components **(table 1)**. In POH…rGO system, there are two POH populations such as free POH and adsorbed POH. So, one can expect two different decay constants, one is for adsorbed POH, which is involve in the electron transfer process and another one is for free POH, which could be entail in the ESPT process. Here, one may raise a question on the observed shorter component with rGO. Since, fluorescence lifetime of rGO is reported in many previous studies[36] and it show multiexponential decay kinetics ranging from 1 ps to 2 ns. However, the rGO material that we have prepared is non-fluorescent in nature; hence it will not affect our time resolved results. Moreover, we have provided the fluorescence decay dynamics of rGO (**Figure 5**) under similar experimental condition. We strongly believe that the observed thermal counts of rGO solution (figure 5) are not affecting our TCSPC data and hence, the observed shorter component is truly due to electron transfer. Therefore, the shorter component (0.11 ns) is assigned to POH adsorbed onto rGO while the longer component (5.2 ns) is assigned to free POH.

It is established previously[37] that the decrease in the fluorescence decay entirely due to electron transfer process. So, the rate of electron transfer (k_{et}) from excited state POH to rGO can be calculated by using the equation (5)

$$k_{et} = 1/\tau_{ads} - 1/\tau_{free} \quad \rightarrow (5)$$

where, τ_{free} & τ_{ads} are the lifetimes of POH in the absence and presence of rGO respectively (table 1). The calculated k_{et} value is 8.8 x 10^9 s^{-1}. On the other hand, the solvent used in the entire studies is water, so free POH may involved in ESPT process. Hence, determination of k_{et} using this τ_{free} is questionable. In principle, one can determine the true k_{et} using τ_{free} as 4.4 ns (fluorescence lifetime measured in ACN medium, since at this solvent no deprotonation occurred, see **figure 4**). The calculated k_{et} is 8.9 × 10^9 s^{-1}, which is very similar with previously calculated k_{et}. This clearly tells that τ_{ads} play key role in calculating the k_{et}. We already stated that, the observed τ_{ads} is true, which is not at all distorted by rGO. Moreover, this k_{et} value is exactly fit on the excited state interactions between ZnO nanoparticles and Graphene Oxide reported by kamat et al.[38] The higher k_{et} value indicates that the electron transfer between POH and rGO is efficient. Such an estimate of the electron transfer rate provides the basis for using rGO based materials for collecting photogenerated electrons.

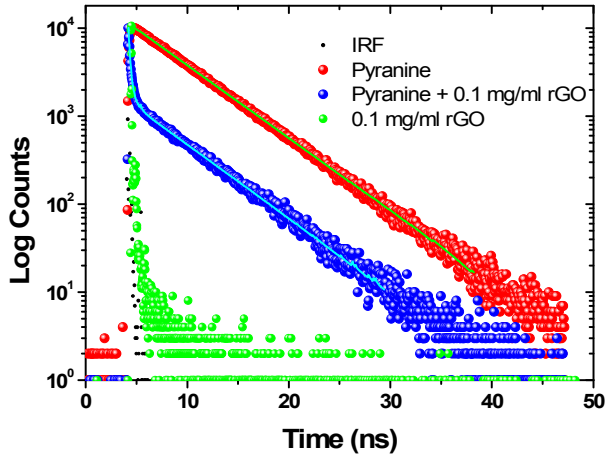

Figure 5: Fluorescence decay dynamics of POH in the absence and presence of rGO.

Table 1: The data of fluorescence lifetime measurements

Sample	τ_{ads} (ns) [A(%)]	τ(ns) [A(%)]	k_{et} × 10^9 s^{-1}
PO^-	--	5.2 [100]	--
PO^-/rGO	0.11 [23]	5.2 [67]	8.8

Thermodynamic consideration

The thermodynamics driving force (ΔG_{et}) of electron transfer between POH and rGO can also be verified according to the well known Rehm–Weller expression (6).[39] The energy balance of a photoinduced electron transfer reaction is given by the Rehm-

Weller equation which combines the oxidation potential (E_{ox}) of the electron donor, the reduction potential (E_{red}) of the electron acceptor, an electrostatic correction term C and the excited state energy of the sensitizer. Therefore, Rehm-Weller equation remains valid for measurements of fluorescence quenching through electron transfer.

$$\Delta G_{et} = E_{1/2}^{oxi} - E_{1/2}^{red} - E_s + C \quad \rightarrow (6)$$

Where, $E_{1/2}^{oxi}$ is oxidation potential of donor (0.42 V), $E_{1/2}^{red}$ is reduction potential of acceptor (–0.85 V),[40] E_s is the excited state energy of POH is 2.41 eV (E_s value is estimated from the florescence maximum) and C is the Coulombic term. Since one of the species is neutral and the solvent used is polar, the coulombic term in the above expression is neglected. The calculated ΔG_{et} value is −1.14 eV. The obtained ΔG_{et} value is highly exothermic and hence, the electron transfer reaction of POH is energetically favorable. A high exothermic of ΔG_{et} is the incontestable proof for the electron-transfer mechanism.

Transient absorption spectroscopy

To get the deeper insights about an electron transfer between POH and rGO, we have employed transient absorption spectroscopy. If electron injection from the excited state of POH to the rGO occurs, the radical cation of POH should be detected. **Figure 6** shows the transient absorption spectrum of POH at 1 µs time delay after excitation at 355 nm. According to following equation (7),[41] the transient absorption spectrum has contributions from the ground state bleaching (GSB), stimulated emission (SE), excited state absorption (ESA) and triplet state absorption (TSA).

$$\Delta A = \Delta A_{ESA} + \Delta A_{TSA} - \Delta A_{GSB} - \Delta A_{SE} \quad \rightarrow (7)$$

The measured transient absorption spectrum has strong contribution from TSA only. Since at this time scale there is no contribution from stimulated emission (SE), because the singlet lifetime of POH is 5.2 ns. The transient absorption spectrum has pronounced band at 440 is assigned to the triplet state absorption in accordance with the earlier observations.[42]

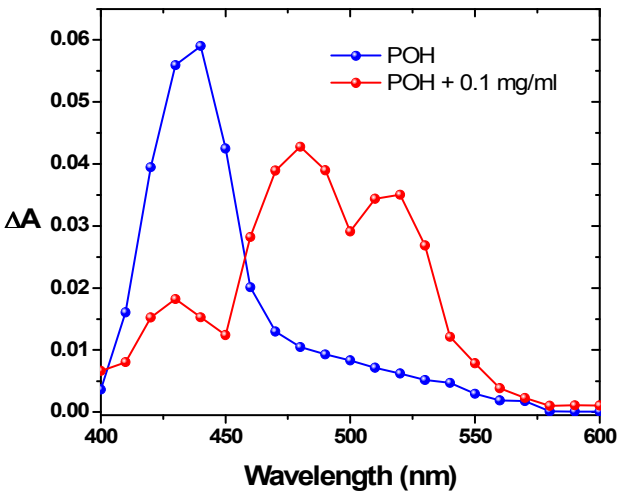

Figure 6: Transient absorption spectra of POH in the absence and presence of rGO at 1µs.

However, in the presence of rGO (0.1 mg/ml) two new bands (470 nm and 510 nm) were observed, moreover the triplet of pyrene is almost quenched. This clearly shows that there is a singlet electron transfer quenching. We assigned the band at 470 nm is due to radical cation of pyrene and band at 510 nm is due to radical anion of graphene. In support to our assignment, Mercedes et al. observed the similar type of bands in the presence of carbon materials.[42] Rao et al. also reported radical anion of graphene for the evidence of photoinduced electron transfer between organic molecules with graphene.[31a] In conclusion, we have provided the direct evidence for the electron transfer quenching of excited POH with rGO. More detailed ultrafast dynamics and photovoltaic performance on real device (pyrene derivatives/rGO/TiO_2) will be explored in near future.

Conclusions

We have analyzed the effect of rGO addition on the spectral properties of POH. Results reveals that, POH can be adsorbed on the surface of rGO dispersion with an apparent association constant of 33.4 $(mg/ml)^{-1}$. Moreover, the fluorescence of POH effectively quenched by rGO. Quenching is due to electron transfer. The rate of electron transfer process from excited singlet state of POH to the rGO dispersion (k_{et}) is 8.8 x 10^9 s^{-1}. The obtained negative ΔG_{et} value suggesting that the electron transfer reaction of POH with rGO is energetically favorable. With laser flash photolysis technique, a direct evidence for the process of electron injection was obtained. The main implication of the present work is to probe the excited state interactions of POH with rGO. Here, rGO acts as an electron acceptor. The ability of rGO is to store and shuttle the electrons, which can be utilized to develop an efficient photoanode (i.e.) dye/rGO/TiO_2 interface[43] for solar energy conversion.

Acknowledgment

A.K. and C.N. thanks to Department of Science and Technology, India for DST-INSPIRE Faculty Award.

Notes

[a] *Department of Chemistry, B.S. Abdur Rahman University, Chennai – 600 048, Tamil Nadu, India*
[b] *Centre for Energy and Environmental Science and Technology, National Institute of Technology, Tiruchirappalli 620 015, Tamil Nadu, India*
[c] *National Centre for Ultrafast Processes, University of Madras, Taramani Campus, Chennai – 600 113, Tamil Nadu, India*

* Author for correspondence
E-mail address: akathir23@hotmail.com (Dr. A. Kathiravan)

Electronic Supplementary Information (ESI) available.

References

1 C.N.R. Rao, A.K. Sood, K.S. Subrahmanyam and A. Govindaraj, *Angew. Chem., Int. Ed.,* 2009, **48**, 7752.

2 K.S. Novoselov, A.K. Geim, S.V. Morozov, D. Jiang, Y. Zhang, S.V. Dubonos, I.V. Grigorieva and A.A. Firsov, *Science*, 2004, **306**, 666.

3 P.V. Kamat, *J. Phys. Chem. Lett.,* 2010, **1**, 520.

4 W.S. Hummers and R.E. Offeman, *J. Am. Chem. Soc.,* 1958, **80**, 1339.

5 G.I. Titelman, V. Gelman, S. Bron, R.L. Khalfin, Y. Cohen and H. Bianco-Peled, *Carbon,* 2005, **43**, 641.

6 A.B. Bourlinos, D. Gournis, D. Petridis, T. Szabo, A. Szeri and I. Dekany, *Langmuir,* 2003, **19**, 6050.

7 Y. Si and E.T. Samulski, *Nano Lett*., 2008, **8**, 1679.

8 V. Yong and J.M. Tour, *Small*, 2010, **6**, 313.

9 Y.B. Tang, C.S. Lee, J. Xu, Z.T. Liu, Z.H. Chen, Z. He, Y.L. Cao, G. Yuan, H. Song, L. Chen, L. Luo, H.M. Cheng, W.J. Zhang, I. Bello and S.T. Lee, *ACS Nano,* 2010, **4**, 3482.

10 H. Hayashi, I.V. Lightcap, M. Tsujimoto, Mi. Takano, T. Umeyama, P.V. Kamat and H. Imahori, *J. Am. Chem. Soc.,* 2011, **133**, 7684.

11 X.F. Zhang and F. Li, *J. Photochem. Photobiol. A Chem.*, 2012, **246**, 8. [references cited therein].

12 X. Zhang and Q. Xi, *Carbon*, 2011, **49**, 3842.

13 (a) A. Baheti, C.P. Lee, K.R.J. Thomas and K.C. Ho, *Phys. Chem. Chem. Phys.,* 2011, **13**, 17210. (b) J. Huang, K. Jiang, C.C. Yu, S. Li, G. Li, L.M. Yang and Y.L. Song, *RSC Adv*., 2014, **4**, 22181.

14 H. Chakraborti, K. Bramhaiah, N.S. John and S.K. Pal, *Phys. Chem. Chem. Phys.,* 2013, **15**, 19932.

15 X. Zhu, Y. Zhu, S. Murali, M. D. Stoller and R.S. Rouff, *ACS Nano* 2011, **5**, 3333.

16 F. Kim, J. Y. Luo, R. Cruz-Silva, L. J. Cote, K. Sohn and J. X. Huang, *Adv. Funct. Mater.,* 2010, **20**, 2867.

17 J. Shen, Y. Hu, M. Shi, X. Lu, C. Qin, C. Li and M. Ye, *Chem. Mater.,* 2009, **21**, 3514.

18 N. A. Kumar, H. J. Choi, Y. R. Shin, D. Chang, L. Dai and J.B. Baek, *ACS Nano*, 2012, **6**, 1715.

19 (a) C. Fu, G. Zhao, H. Zhang and S. Li, *Int. J. Electrochem. Sci.*, 2013, **8,** 6269. (b) W. Gao, L.B. Alemany, L. Ci and P.M. Ajayan, *Nat. Chem.,* 2009, **1**, 403. (c) Z.S. Wu, W. Ren, L. Wen, L. Gao, J. Zhao, Z. Chen, G. Zhou, F. Li and H.M. Cheng, *ACS Nano,* 2010, **4**, 3187.

20 C. N. R. Rao, K. Biswas, K. S. Subramnayam and A. Govindaraj, *J. Mater. Chem.,* **2009**, 19, 2457.

21 J. Zhu, T. Zhu, X. Zhou, Y. Zhang, X. W. Lou, X. Chen, H. Zhang, H. H. Hng and Q. Yan, *Nanoscale,* 2011, **3**, 1084.

22 Y. Wang, D.C. Alsmeyer and R. McCreery, *Chem. Mater.,* 1990, **2**, 557.

23 M.S. Dresselhaus, Phil. Trans. R. Soc. A 2008, **366,** 189.

24 J. Shen, Y. Hu, M. Shi, X. Lu, C. Qin, C. Li and M. Ye, *Chem. Mater.,* 2009, **21**, 3514.

25 G. Wang, X. Chen, B. Wang, J. Yao and J. Park, *Carbon*, 2009, **47**, 2049.

26 L. G. Cancado, A. Reina, J. Kong and M.S. Dresselhaus, *Phys. Rev. B* 2008, **77**, 245408.

27 (a) T.H. Tran-Thi, T. Gustavsson, C. Prayer, S. Pommeret and J.T. Hynes, *Chem. Phys. Lett*., 2000, **329,** 421. (b) S.K. Mondal, K. Sahu, P. Sen, D. Roy, S. Ghosh and K. Bhattacharyya, *Chem. Phys. Lett*., 2005, **412,** 228. (c) K. Sahu, D. Roy, S.K. Mondal, R. Karmakar and K. Bhattacharyya, *Chem. Phys. Lett*., 2005, **404,** 341. (d) S.K. Mondal, S. Ghosh, K. Sahu, P. Sen and K. Bhattacharyya, *J. Chem. Sci*., 2007, **119,** 71. (e) D. Roy, R. Karmakar, S.K. Mondal, K. Sahu and K. Bhattacharyya, *Chem. Phys. Lett*., 2004, **399,** 147.

28 (a) A. Suwaiyan, F. Al-adel, A. Hamdan and U.K.A. Klein, *J. Phys. Chem*., 1990, **94,** 7423. (b) J. Lee, R.D. Grin and G.W. Robinson, *J. Chem. Phys*., 1985, **82,** 4920. (c) E. Pines and G.R. Fleming, *J. Phys. Chem*., 1991, **95,** 10448. (d) N. Agmon, D. Huppert, A. Masad and E. Pines, *J. Phys. Chem*., 1991, **95,** 10407.

29 (a) J. Geng and H.T. Jung, *J. Phys. Chem. C*, 2010, **114**, 8227. (b) Y. Xu, H. Bai, G. Lu, C. Li and G. Shi, *J. Am. Chem. Soc.* 2008, **130**, 5856.

30 H.A. Benesi, J.H. Hildebrand, *J. Am. Chem. Soc.*, 1949, **71,** 2703.

31 (a) H.S.S. Ramakrishna Matte, K.S. Subrahmanyam, K. Venkata Rao, Subi J. George and C.N.R. Rao, *Chem. Phys. Lett*., 2011, **506**, 260. (b) M. Miguel, M. Álvaro and H. García, *Langmuir*, 2012, **28**, 2849.

32 (a) S. Anandan and M. Yoon, *Spectrochim. Acta A,* 2004, **60**, 885.(b) A. Kathiravan and R. Renganathan, *J. Colloid and Interface Sci.*, 2009, **335**, 196. (c) M. Asha Jhonsi, A. Kathiravan and R. Renganathan, *J. Lumin.,* 2009, **129**, 854.

33 (a) E.B. de Borba, C.L.C. Amaral, M. J. Politi, R. Villalobos and M. S. Baptista, *Langmuir*, 2000, **16**, 5900. (b) C. Prayer, T.H. Tran-Thi, S. Pommeret, P. d'Oliveira and P. Meynadier, *Chem. Phys. Lett*., 2000, **323**, 467.

34 S.E. Koops and J.R. Durrant, *Inorg. Chim. Acta,* 2008, **361**, 663.

35 (a) A. Reynal, A. Fornelia and E. Palomares, *Energy Environ. Sci.,* 2010, **3**, 805. (b) A. Reynal, A. Forneli, E.M. Ferrero, A.S. Dıaz, A.V. Ferran, B.C. O'Regan and E. Palomares, *J. Am. Chem. Soc.*, 2008, **130**, 13558. (c) H.J. Snaith, A. Petrozza, S. Ito, H. Miura and M. Grätzel, *Adv. Funct. Mater.,* 2009, **19**, 1810. (d) J. Chen, Y. Zou, Y. Li, X. Zhou, J. Zhang, X. Li, X. Xiao, Y. Lin, *Chem. Phys. Lett.,* 2008, **460**, 168.

36 (a) J. Shang, L. Ma, J. Li, W. Ai, T. Yu, G.G. Gurzadyan, *Sci. Rep*., 2012, **2**, 792. (b) D. Kozawa, Y. Miyauchi, S. Mouri, K. Matsuda, *J. Phys. Chem. Lett*., 2013, **4**, 2035. (c) C. Chien, S.S. Li, W.J. Lai, Y.C. Yeh, H. Chen, I. Chen, L.C. Chen, K.H. Chen, T. Nemoto, S. Isoda, M. Chen, T. Fujita, G. Eda, H. Yamaguchi, M. Chhowalla, C.W. Chen, *Angew. Chem. Int. Ed*., 2012, **51**, 6662. (d) S. Kaniyankandy, S.N. Achary, S. Rawalekar, H.N. Ghosh, *J. Phys. Chem. C*, 2011, **115**, 19110.

37 (a) P**.** V. Kamat, J. P. Chauvet, R. W. Fessenden, *J. Phys. Chem*., 1986, **90**, 1389. (b) P. V. Kamat, *J. Phys. Chem*., 1989, **93**, 859. (c) C.Y. Wang, C.Y. Liu, W.Q. Wang, T. Shen, *J. Photochem. Photobiol. A: Chem*., 1997, **109**, 159. (d) C. Chen, X. Qi, B. Zhou, *J. Photochem. Photobiol. A: Chem*., 1997, **109**, 155. (e) J. He, F. Chen, J. Zhao, H. Hidaka, *Colloids and Surfaces A*, 1998, **142**, 49. (f) Z.X. Zhou, S.P. Qian, S.D. Yao, Z.Y. Zhang, *Dyes and Pigments*, 2001, **51**, 137. (g) Z. Zhou, S. Qian, S. Yao, Z.A. Zhang, *Radiat. Phys. Chem*., 2002, **65**, 241. (h) A. Listorti, I.L. Duarte, M.V. M. Diaz, T. Torres, T. DosSantos, P.R.F. Barnes, J.R. Durrant, *Energy Environ. Sci*., 2010, **3**, 1573.

38 G. Williams and P.V. Kamat, *Langmuir,* 2009, **25**, 13869.

39 D. Rehm and A.Weller, *Isr. J. Chem*., 1970, **8**, 259.

40 D. Chen, L. Tang and J. Li, *Chem. Soc. Rev.,* 2010, **39**, 3157.

41 H. Imahori, S. Kang, H. Hayashi, M. Haruta, H. Kurata, S. Isoda, S.E. Canton, Y. Infahsaeng, A. Kathiravan, T. Pascher, P. Chabera, A.P. Yartsev and V. Sundstrom, *J. Phys. Chem. A* 2011, **115**, 3679.

42 M. Alvaro, P. Atienzar, J.L. Bourdelande and H. Garcia, *Chem. Phys. Lett*. 2004, **384**, 119.

43 (a) M. Zhu, X. Li, W. Liu and Y. Cui, *J. Power Sources,* 2014, **262**, 349. (b) J. Zhao, J. Wu, F. Yu, X. Zhang, Z. Lan and J. Lin, *Electrochimica Acta*, 2013, **96**, 110.